THE SIMULATION OF THE BEHAVIOUR OF ALLOYING ADMIXTURE PARTICLES IN THE INDUCTION CRUCIBLE FURNACES

M. Ščepanskis[(1)], A. Jakovičs[(1)], B. Nacke[(2)] and E. Baake[(2)]

[1]Laboratory for Mathematical Modelling of Environmental and Technological Processes, University of Latvia
Zellu str. 8, LV-1002 Riga, Latvia

[2]Institute of Electrotechnology, Leibniz University of Hanover
Wilhelm-Busch-str. 4, 30167 Hanover, Germany

ABSTRACT. The process of electromagnetic mixing of alloying admixtures in the metal melt is simulated in the present paper. The simulation of the EM induction governed a turbulent flow is carried out using the Large Eddy Simulation (LES) method with the Smagorinsky subgrid viscosity model. The motion of the admixture particles is simulated using the Lagrangian equation that takes into account drag, buoyancy, EM, lift, acceleration and added mass forces. The influence of the different forces on the particle trajectory is analyzed and the progress of the process of the admixtures homogenization for particles with different diameter is investigated. The typical time of the homogenization is also estimated.

INTRODUCTION

The different alloying particles are mixed into the steel melt to increase some properties, such as strength, hardness, wear resistance and others. The different chemical elements, that are used as alloying admixtures, and their densities are shown on Table 1. The density of the alloy steel ranges between 7.75 and $8.05\,g/cm^3$ (it depends on the alloying constituents). Thus there are the admixtures with higher and lighter densities then the steel density.

Table 1. The densities of alloying elements.

chemical element	density, g/cm^3
molybdenum (Mo)	10.28
nickel (Ni)	8.908
manganese (Mn)	7.21
chromium (Cr)	7.19
vanadium (V)	6.0
silicon (Si)	2.3290
boron (B)	2.08

Table 2. The properties of laboratory scale ICF.

property	value
inductor frequency	365 Hz
inductor current	2000 A
melt height, inductor height	570 mm
crucible radius	158 mm
number of inductor turns	12

It is important to rich the homogeneous admixtures distribution to ensure a high quality of the alloy. To estimate the time of the homogenization the model of the motion of the admixture particles is created.

The simulation is carried out for the model of the cylindrical induction crucible furnace (ICF) which is typical object for the inductive melting processes. The sketch of ICF is shown on Figure 1 and the sizes and other parameters are shown on Table 2. The laboratory ICF with such parameters was used in some previous theoretical and experimental investigations (for example in [1, 2]), therefore we also use this ICF to have the possibility to compare the results. For the same reason the flow of the Wood's metal is considered.

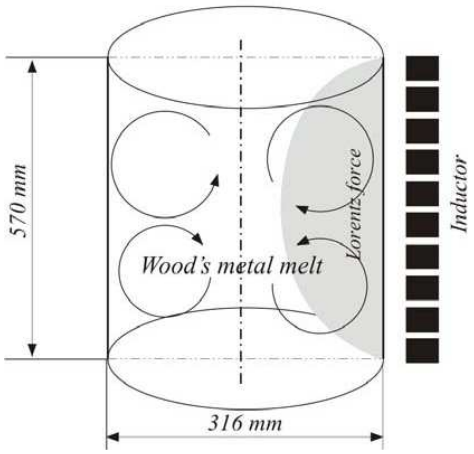

Figure 1. The design of ICF with the sketch of the typical vortices of the mean flow.

THEORETICAL ANALYSIS AND MODEL

The numerical simulation is carried out using a free code *OpenFOAM* software.

Present model includes the flow and the particle motion simulation. The turbulent flow simulation is carried out using the LES method with the Smagorinsky subgrid viscosity model [2]. The flow is governed by electromagnetic force and thermal buoyancy force in the Boussinesq approximation [2]. The adiabatic and the convective thermal boundary conditions were considered.

The time step 0.005 s is used in calculations; the mesh has about 3 million elements; the typical time of the calculation of 10 s on 1 processor is about 3 days.

The result of the flow simulation is the field of the flow velocities at each time step that is used for the particle trajectories calculation. The Lagrangian equation describes the motion of the particles.

The theoretical investigation of the particle motion

Let us initially consider a movable spherical particle in a still liquid. This case is same as the case when the liquid moves and the particle is immovable. The non-stationary Navier-Stokes equation that describes the motion of the liquid:

$$\frac{\partial \mathbf{u_f}}{\partial t} = -\frac{1}{\rho} \cdot \nabla p + \nu \cdot \Delta \mathbf{u_f}, \qquad (1)$$

where $\mathbf{u_f}$ is velocity of the flow (the origin of the flow motion is only the motion of the particle), p is pressure, ρ is density, ν is kinematic viscosity.

Using *curl* operator we can get rid of the pressure in Eq. 1 [3] and write this equation for a flow function ψ in a spherical coordinate system [4, 5]:

$$\left(L-\frac{1}{\nu}\frac{\partial}{\partial t}\right)L\psi=0, \tag{2}$$

where $L=\frac{\partial^2}{\partial r^2}+\frac{\sin\theta}{r^2}\frac{\partial}{\partial\theta}\left(\frac{1}{\sin\theta}\frac{\partial}{\partial\theta}\right)$ is differential operator. The boundary conditions are

$$\frac{1}{a^2\sin\theta}\frac{\partial\psi}{\partial\theta}=u_p(t)\cdot\cos\theta, \qquad \frac{1}{a\sin\theta}\frac{\partial\psi}{\partial r}=u_p(t)\cdot\sin\theta,$$

where $u_p(t)$ is velocity of the particle, a is the radius of the particle.

Eq. 2 is solved using the Laplace transformation [6] for non-slip boundary conditions [4, 5], and force $\mathbf{F}$ on the spherical particle obtained by evaluating the stress on the surface and integrating is as follows [4]:

$$\frac{\mathbf{F}}{\rho\cdot V_p}=-\frac{1}{2}\frac{d\mathbf{u_p}}{dt}+\frac{3}{2}\frac{d\mathbf{u_f}}{dt}+\frac{9\nu}{2a^2}\cdot\left(\mathbf{u_f}-\mathbf{u_p}\right)+\frac{9}{2a}\sqrt{\frac{\nu}{\pi}}\cdot\int_0^t\frac{d\left(\mathbf{u_f}-\mathbf{u_p}\right)}{d\tau}\frac{d\tau}{\sqrt{t-\tau}}. \tag{3}$$

We can compare Eq. 3 with result obtained for potential liquid and generalize it by replacing $\frac{d\mathbf{u_f}}{dt}$ to $\frac{D\mathbf{u_f}}{Dt}$, where $\frac{D}{Dt}$ is material derivation [4, 7].

The summand that contains the integral in Eq. 3 is too complex for numerical modeling while its contribution to the force is not so big because of the oscillation of the flow acceleration [2].

It is necessary to note that the flow in our case is not the Stokes flow. The Reynolds number for the particles $\mathrm{Re}_p=aU/\nu$ was estimated [2] ($U=u_f-u_p$). Acceleration parameter $Ac=U^2\big/a\dot{U}$ ($\dot{U}$ is relative acceleration) was also estimated. Taking into account these estimations we should change the coefficients in some summands in Eq. 3. The Schiller-Naumann approximation for the drag coefficient C_D [8] and the Odar-Hamilton approximation for acceleration coefficient C_A [9] are used.

The density of the liquid ρ_f and the density of the particles ρ_p are different, so we should take into account buoyancy force. There is EM field that influence the motion of the particle, so we also should take into account EM force. Lift force appears due to the flow circulation and is significant in some regions of the crucible. The Legendre-Magnaudet approximation for the lift coefficient C_L [10] is used.

Thus the Lagrangian equation for non-conductive particle motion is so:

$$\left(1+\frac{C_A}{2}\frac{\rho_f}{\rho_p}\right)\cdot\frac{d\mathbf{u_p}}{dt}=C_D\cdot\mathbf{U}+\left(1-\frac{\rho_f}{\rho_p}\right)\cdot\mathbf{g}-\frac{3}{4}\frac{1}{\rho_p}\mathbf{f_{em}}+\frac{\rho_f}{\rho_p}C_L\xi+\left(1+\frac{C_A}{2}\right)\cdot\frac{D\mathbf{u_f}}{Dt}, \tag{4}$$

where coefficients C_D, C_L and C_A depends on Re_p; vector $\mathbf{f_{em}}=[\mathbf{j}\times\mathbf{B}]$ is the Lorentz force density, $\mathbf{j}$ is a current density, $\mathbf{B}$ is magnetic field induction; vector $\xi=[\mathbf{U}\times[\nabla\times\mathbf{U}]]$ describes the lift force.

The structure of Eq. 4 is following:

$$\left[\frac{d\mathbf{u_p}}{dt} + added\ mass\ 1\right] = [drag] + [buoyancy] + [EM] + [lift] + [acceleration + added\ mass\ 2].$$

The added mass force is divided in two parts (*added mass 1* and *added mass 2*) like it is implemented in the algorithm.

The algorithm of the simulation

The first step of numerical algorithm is the fluid velocity field calculation; the second one is the particles motion simulation. Both steps are implemented at each time step.

We consider particle transport model with several assumptions made:

- the particle-particle interaction is negligible,
- all particles are rigid spheres,
- the particles do not affect the structure and the velocities of the flow,
- the particles can slide along the wall but cannot stick to the wall (the processes of the surface diffusion and the deformation of the particle are not considered).

Eq. 4 is solved numerically using the implicit difference scheme. Thus we get the system of linear algebraic equation for vector $\mathbf{u_p}$ components. This system is solved using Gauss method.

RESULTS OF SIMULATION

The particles are input in the developed turbulent flow in a plane near the top surface of the crucible (1.5 cm deep). This particle initial distribution qualitatively corresponds to the industrial case of the admixture components inputting in a melt.

The analysis of the influence of the different forces on the particle trajectory

The number of numerical experiments was carried out taking into account different forces. Using the results of the experiments the influence of these forces on particle motion in the turbulent EM induced flow was analyzed.

Drag force is basic reason of the particle motion. The particle is accelerated when the flow velocity is more than the particle one. The less the size of the particle, the bigger is drag force, thus the motion of the small particles repeats the flow motion. The greater particles have more inertia and react to the changes of the flow velocity more slowly. The dependence of drag force on the particle size is not linear. This is the only force that divided to the mass significantly depends on the size of the particle.

EM force is significant in the skin layer near the side wall of the crucible. Then the non-conductive particle comes to this layer the EM force try to move it in the direction of the wall. If we are comparing the trajectories of the particle then for the one EM force is taken into account and for the other is not taken then we can see that due to EM force the trajectories separate near the wall, particles come to different flow conditions and their further trajectories are totally different.

Lift force is significant in the areas where both velocity magnitude and derivative of velocity magnitude are significant. Such stationary areas are situated near the wall of the crucible in the zones of the eddies (Figure 4 (a)) In a thin layer near the wall the velocity reaches maximum and the border condition for velocity is $\mathbf{u_f} = 0$. Thus the area derivative of the velocity has different sign in different directions from the point of the velocity maximum $r_{\max}$. Lift force tries to move the particle away from the wall if it is very close to the wall ($r > r_{\max}$), and moves it to the wall if it is in the opposite side of the point ($r < r_{\max}$), where

the velocity reaches the maximum. Due to non-stationary turbulent flow simulation some short-term areas, where the lift force is significant, also appears inside of the crucible. When the particle comes to this area, lift force changes its trajectory.

Due to non-stationary turbulent flow, areas with significant flow acceleration also transiently appear. Thus acceleration and added mass forces influences the particle motion too.

The examples of trajectories of particles, when some forces are taken into account and not taken, are shown on Figure 2. On (a) and (c) we can see that due to lift, acceleration and added mass forces the particle comes to the lower part of crucible. Thus all mentioned forces are significant and can considerably change the trajectory of the particle.

The particles with different density and size

As it is shown on Table 1 there are some alloying elements with density more than steel density, some with lower density and some with density close to steel density. Therefore we consider 3 typical cases: $\rho_p = \rho_f / 1.5$, $\rho_p = \rho_f$ and $\rho_p = 1.5 \cdot \rho_f$.

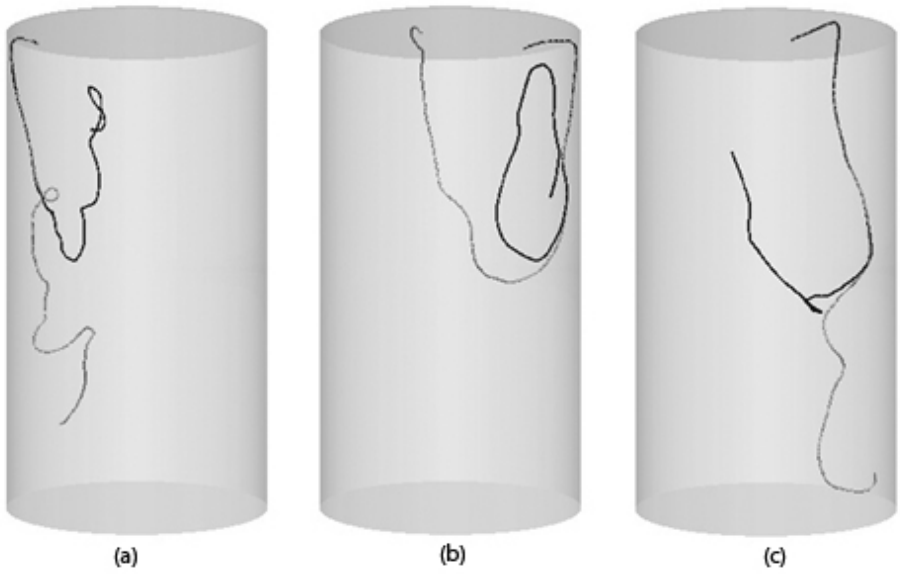

Figure 2. The trajectories of the particle taking into account different forces: dark colure trajectory – drag and EM forces; light colure trajectory – drag, EM, lift, acceleration and added mass forces.

In the case of heavy particles (Figure 3 (c)) big particles rapidly come to the bottom of the crucible and only some small particles are moving in the flow. It can be explained with fact that the drag force for small particles has large magnitude than the buoyancy one.

In the cases of the particles with density equal and less than liquid density also only small particle can move in the flow. Big particles with the density equal to the density of the liquid are concentrated in the middle zone of the crucible near the wall (Figure 3 (b, e)). This is the zone between two eddies of the averaged flow, thus the velocity of the liquid is low in the middle of the crucible and particles can stay there. The EM force presses the particles to the wall, thus they are concentrated near the wall. The same situation we can see in the case of the light particles (Figure 3 (a, d)). But due to buoyancy force some particles remain on the top surface of the melt and form the “slag” that is also observed in industrial furnaces [11].

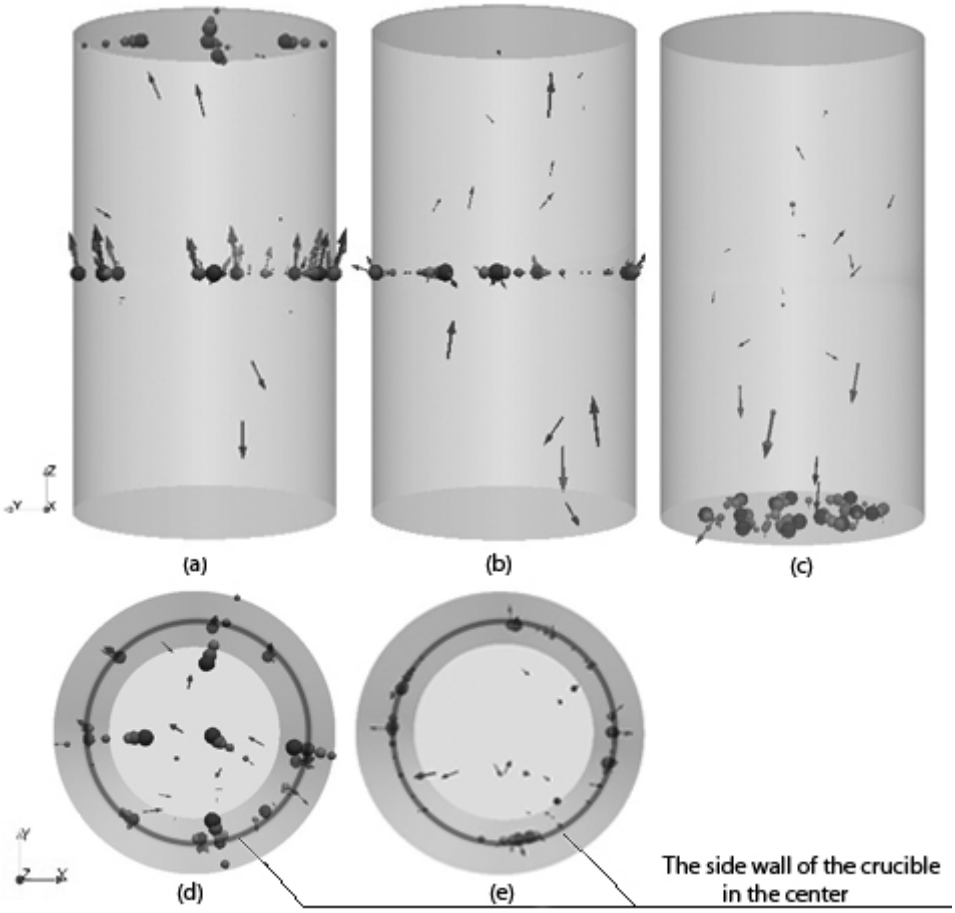

Figure 3. The positions of the particles in ICF after 7 s from the moment than they was input. The diameter of the particles ranges between 0.1 and 1.9 mm. (a), (d) - $\rho_p = \rho_f / 1.5$, (b), (e) - $\rho_p = \rho_f$, (c) - $\rho_p = 1.5 \cdot \rho_f$. The arrows show the direction and the magnitude of the momentary particle velocity at the 7 s. The images are drawn with respect to the optical perspective.

We can make the conclusion that for these parameters of ICF and considered densities only the particles with diameter less than 0.3 mm are moving in the flow. Thus for same ICF we should consider only the particles with such diameters in further investigations.

The homogenization of the alloying particles

The process of homogenization of alloying particles is considered for about $3 \cdot 10^4$ particles with different diameter and $\rho_p = \rho_f / 1.5$. Figure 3 (a) shows the field of the average flow velocity in the central vertical plane of the crucible. The boxes show the areas of the upper and the lower eddies where the number of the particles is analyzed. The middle zone between the upper and the lower eddies is the zone where small eddies appear, thus the particle in this zone hesitates and goes to the upper or the lower eddies. If the particle comes to the layer near the wall, where EM force is significant, it can stay in this zone due to the EM force. Analyzing the results of the simulation we can note that the significant number of the particles with diameter 0.2 mm is concentrated near the wall in the middle zone and does not go into the flow.

The process of homogenization take place between the zones of two eddies; therefore the difference between the number of the particles in the zone of the upper eddy and the one in

the zone of the lower eddy is analyzed. The results of simulation show that the radial and angular distributions of the particles in the crucible rapidly became homogeneous.

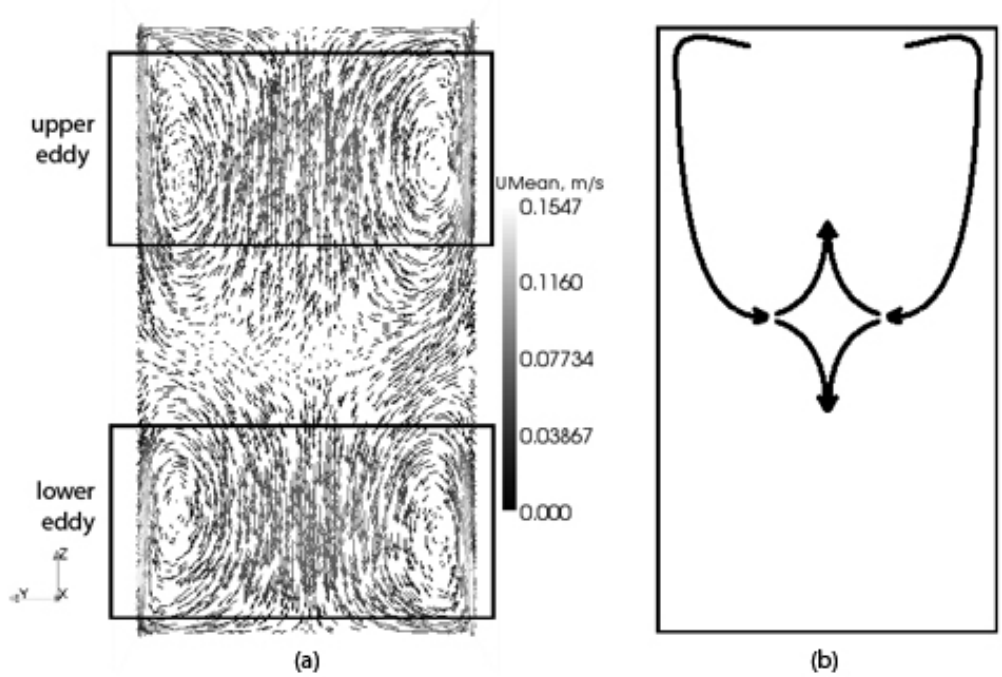

Figure 4. (a) – the average flow velocity in the central vertical plane in ICF; (b) – the scheme of the motion of the particle cloud in ICF.

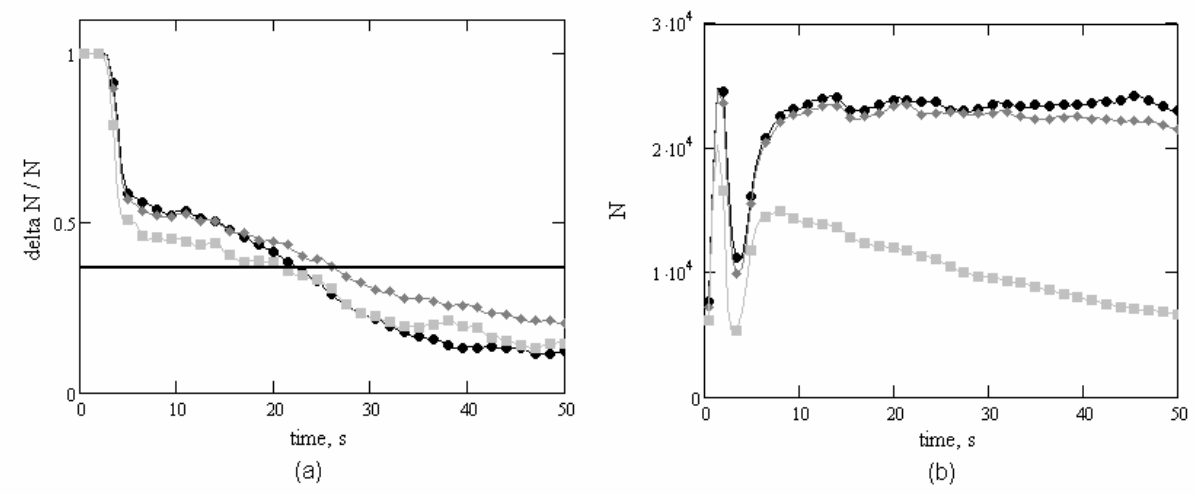

Figure 5. (a) - the evolution of the relative difference between the number of the particles in the zones of the upper and lower eddies. (b) – the number of particles in both zones. The particles with different diameter: ●●●0.05 mm; ◆◆◆0.1 mm; ■■■0.2 mm.

Figure 4 (b) schematically shows the motion of the particles cloud. Initially all particles are going down through the zone of the upper eddy near the wall to the middle part. Then the cloud of the particles separates: one part goes to the zone of the upper eddy and other part to the zone of the lower eddy. After that the particle exchange between two eddies decreases the difference between the number of the particles in zones of the upper and the lower eddies ΔN with the lapse of time. Figure 5 (a) shows the evolution of ΔN, normalized with respect to the number of the particles in the both zones, for the particles with different diameter.

We can define the time of the homogenization of the alloying particles t_e as the time when $\Delta N/N$ decreases e times. The time of homogenization t_e in the analyzed cases ranges between 21 and 26 s. It takes about 3 s for the cloud of the particles to come from the surface to the middle zone between the eddies in the analyzed flow with maximal velocities 15 cm/s. The minimum of N appears at this time (Figure 5 (b)). The particle number in the lower and the upper eddies does not become equal due to the low density of the particles, but $\Delta N/N$ stabilizes at the level of 25%. N also stabilizes for the particles with the diameter 0.05 and 0.1 mm (Figure 5 (b)). Analyzing the results of the simulation we can conclude that the number of the particles with the diameter 0.2 mm that concentrate in the middle zone near the wall grown up with the lapse of time, thus the number of particles that moves in the flow and are calculated in $\Delta N/N$ on Figure 5 (a) decreases

CONCLUSIONS

The model of the particle transportation in the turbulent flow of ICF is proposed in this paper. The influence of different forces (drag, buoyancy, EM, lift, acceleration and added mass) on the particle motion was analyzed. The motion of the alloying particles with different density and sizes is simulated and the critical diameter when the particles come into the flow for the typical laboratory scale ICF is obtained. The process of the homogenization of the alloying particles is analyzed and the characteristics of the homogenization for the particles with different diameter are estimated.

REFERENCES

[1] M. Kirpo, A. Jakovics, B. Nacke and E. Baake (2008). Particle transport in recirculated liquid metal flows. *COMPEL The International Journal for Computation and Mathematics in Electrical and Electronic Engineering,* 27(2), 377-386.

[2] M. Kirpo (2009). *Modeling of turbulence properties and particle transport in recirculated flows (PhD thesis)*. University of Latvia, Faculty Physics and Mathematics, Department of Physics, Riga

[3] L. E. Landau and E. M. Lifshitz (1959). *Fluid mechanics.* Pergamon, New York.

[4] C. E. Brennen (2005). *Fundamentals of multiphase flow*. Cambridge University Press, New York.

[5] A. B. Basset (1888). *A treatise on hydrodynamics with numerous examples. Vol. II.* Deighton, Bell and Co, Cambridge.

[6] M. A. Lavrent'ev and B. V. Shabat (1973). *Metody teorii funkciy kompleksnogo peremennogo.* Nauka, Moscow.

[7] C. T. Crowe, M. Sommerfeld and Y. Tsuji (1998). *Multiphase flows with droplets and particles.* CRC Press, Boca Raton.

[8] L. Schiller and Z. Naumann (1933). *Uber die grundlegenden berechnungen bei der schwerkrafttaufbereitung.* Ver. Deut. Ing., 77, 318-320.

[9] F. Odar and W. S. Hamilton (1964). *Forces on a sphere accelerating in a viscous fluid.* J. Fluid Mech, 18, 302.

[10] D. Legendre and J. Magnaudet (1998). *The lift force on a spherical bubble in a viscous linear shear flow*. J. Fluid Mech, 368, 81-126.

[11] E. Dötsch (2009). *Inductive melting and holding.* Vulkan-Verlag, Essen.